

Title	Benzalkonium Chloride Accelerates the Formation of the Amyloid Fibrils of Corneal Dystrophy-associated Peptides
Author(s)	Kato, Yusuke; Yagi, Hisashi; Kaji, Yuichi; Oshika, Tetsuro; Goto, Yuji
Citation	Journal of Biological Chemistry. 288(35) P.25109-P.25118
Issue Date	2013-08
Text Version	publisher
URL	<a href="http://hdl.handle.net/11094/71280">http://hdl.handle.net/11094/71280</a>
DOI	10.1074/jbc.M113.477695
rights	
Note	

***Osaka University Knowledge Archive : OUKA***

<https://ir.library.osaka-u.ac.jp/repo/ouka/all/>

# Benzalkonium Chloride Accelerates the Formation of the Amyloid Fibrils of Corneal Dystrophy-associated Peptides\*

Received for publication, April 15, 2013, and in revised form, July 11, 2013. Published, JBC Papers in Press, July 16, 2013, DOI 10.1074/jbc.M113.477695

Yusuke Kato<sup>†1</sup>, Hisashi Yagi<sup>†1</sup>, Yuichi Kaji<sup>§</sup>, Tetsuro Oshika<sup>§</sup>, and Yuji Goto<sup>‡2</sup>

From the <sup>†</sup>Institute for Protein Research, Osaka University, Yamadaoka 3-2, Suita, Osaka 565-0871, Japan and the <sup>§</sup>Department of Ophthalmology, Institute of Clinical Medicine, University of Tsukuba, Tennoudai 1-1-1, Tsukuba, Ibaraki 305-8575, Japan

**Background:** Formation of amyloid fibrils is accelerated by surfactants such as sodium dodecyl sulfate.

**Results:** Fibrillation of corneal dystrophy-associated peptides was accelerated by benzalkonium chloride, a cationic surfactant widely used in eye drops.

**Conclusion:** The results suggest the potential risk that benzalkonium chloride in eye drops may accelerate amyloid fibrillation.

**Significance:** The results support the view of amyloids that most proteins contain amyloidogenic sequences.

Corneal dystrophies are genetic disorders resulting in progressive corneal clouding due to the deposition of amyloid fibrils derived from keratoepithelin, also called transforming growth factor  $\beta$ -induced protein (TGFBI). The formation of amyloid fibrils is often accelerated by surfactants such as sodium dodecyl sulfate (SDS). Most eye drops contain benzalkonium chloride (BAC), a cationic surfactant, as a preservative substance. In the present study, we aimed to reveal the role of BAC in the amyloid fibrillation of keratoepithelin-derived peptides *in vitro*. We used three types of 22-residue synthetic peptides covering Leu110–Glu131 of the keratoepithelin sequence: an R-type peptide with wild-type R124, a C-type peptide with C124 associated with lattice corneal dystrophy type I, and a H-type peptide with H124 associated with granular corneal dystrophy type II. The time courses of spontaneous amyloid fibrillation and seed-dependent fibril elongation were monitored in the presence of various concentrations of BAC or SDS using thioflavin T fluorescence. BAC and SDS accelerated the fibrillation of all synthetic peptides in the absence and presence of seeds. Optimal acceleration occurred near the CMC, which suggests that the unstable and dynamic interactions of keratoepithelin peptides with amphipathic surfactants led to the formation of fibrils. These results suggest that eye drops containing BAC may deteriorate corneal dystrophies and that those without BAC are preferred especially for patients with corneal dystrophies.

The deposition of amyloid fibrils is associated with amyloidoses, including Alzheimer disease, dialysis-related amyloidosis, and corneal dystrophy (1–5). Although an increasing amount of information on amyloid proteins and their precursors has accumulated with the advent of analytical methods, the molecular

mechanisms underlying the formation of amyloid fibrils (*i.e.* amyloid fibrillation) and developing amyloidoses are still unclear. Corneal dystrophy, one form of amyloidoses, is a group of disorders characterized by the primary, inherited, and progressive opacity of both corneas (1, 4). In advanced cases, patients become blind. Although the several treatments for corneal dystrophy including corneal transplantation are known, recurrence of the disease is inevitable. Genetic analysis has revealed that mutations in keratoepithelin, an extracellular matrix protein that is composed of 683 amino acids and is folded into four constitutive domains, are responsible for several corneal dystrophies (Fig. 1) (1, 4). Keratoepithelin is also known as the transforming growth factor  $\beta$ -induced protein (TGFBI).<sup>3</sup> The three-dimensional structure of keratoepithelin, except for one domain, has not yet been identified (Fig. 1). On the other hand, it is likely that, instead of the whole protein molecule, the fragments of keratoepithelin produced after partial proteolysis may be responsible for amyloid fibrillation, although the details are unclear.

Hereditary corneal dystrophies are characterized by the abnormal deposition of amyloid fibrils and/or granular aggregation in the cornea (6–9). Population analyses have revealed two hot spots of mutation at R124 and R555 (7, 10). The position of R124 in particular has four different mutations that lead to distinct phenotypes: R124C (lattice corneal dystrophy type I), R124H (granular corneal dystrophy type II, also called Avelino type), R124L (granular corneal dystrophy type III), and R124S (granular corneal dystrophy type I). Although keratoepithelin is expressed throughout the body, including the skin, conjunctiva, and kidneys, the deposition of amyloid fibrils has been observed in the cornea only (11). Furthermore, the intrinsic and extrinsic risk factors that accelerate corneal dystrophies are unknown.

Previously, Schmitt-Bernard *et al.* (8) studied the amyloidogenicity of a synthetic 22-residue peptide covering Leu-110—

\* This work was supported by the Ministry of Education, Science, Sports, and Culture, Grant for Scientific Research, 22810014 (2010–2011), 24370067 (2012–2015), and 24592618 (2012–2015), Japan and by the Takeda Science Foundation.

<sup>†</sup> Both authors contributed equally to this work.

<sup>2</sup> To whom correspondence should be addressed: Institute for Protein Research, Osaka University, Yamadaoka 3-2, Suita, Osaka 565-0871, Japan. Tel.: 81-6-6879-8614; Fax: 81-6-6879-8616; E-mail: ygoto@protein.osaka-u.ac.jp.

<sup>3</sup> The abbreviations used are: TGFBI, transforming growth factor  $\beta$ -induced protein; C-, H-, and R-type peptides: 22-residue synthetic peptides covering Leu-110—Glu-131 of the keratoepithelin sequence with Arg124Cys, Arg124His mutations, and wild-type Arg124, respectively; ANS, 8-anilino-1-naphthalenesulfonic acid; BAC, benzalkonium chloride; CMC, critical micelle concentration; ThT, thioflavin T; TEM, transmission electron microscopy.

## BAC Induced Keratoepithelin Fibrillation

Glu-131 of the keratoepithelin sequence and its mutants: R124C (C-type) and R124H (H-type) peptides. The results indicated that these mutations enhanced the amyloidogenicity of the wild-type peptide (R-type), which implied an underlying mechanism of R124 mutation-linked corneal dystrophies.

In addition to the intrinsic amyloidogenicity determined by the amino acid sequence, various extrinsic factors such as pH, solvents, metal ions, membranes, and surfactants affect amyloidogenicity (12, 13). Moreover, the exposure of amyloidogenic regions by denaturation is essential to induce their fibrillation (14–17). Among various surfactants, sodium dodecyl sulfate (SDS), an anionic surfactant, is most widely used as an inducer of amyloid fibrils *in vitro* (18–22). SDS above the critical micelle concentration (CMC) was shown to denature proteins, where SDS micelles accommodated denatured proteins so as to increase their solubility (23). Such high concentrations of SDS were also shown to depolymerize preformed amyloid fibrils. Upon denaturation or depolymerization by SDS above CMC, denatured proteins assumed an open  $\alpha$ -helical conformation, in which interactions between  $\alpha$ -helices were weak (23, 24).

Recently, the effects of SDS mimicking some characteristics of lipids constituting biological membranes (22, 23) on accelerating the amyloid fibrillation at around or slightly below CMC have been reported (18–22). In our previous study, we showed that the amyloid fibrillations of the C-type and H-type peptides were accelerated by low concentrations of SDS slightly below CMC (25). However, the pathological significance of SDS in amyloidoses is unclear because SDS does not exist in the human body.

Here, benzalkonium chloride (BAC), a cationic surfactant, may be clinically important in the pathogenesis of corneal dystrophies. In most commercially available eye drops, various antiseptic reagents, including methyl 4-hydroxybenzoate, ethyl 4-hydroxybenzoate, and BAC, are added, among which BAC is the most widely used (26). Patients with corneal dystrophies frequently use eye drops because of corneal irritation and inflammation, which exposes their corneas to BAC more than others. Considering the marked effects of SDS on the fibrillation of keratoepithelin-derived peptides (25), we anticipated similar effects from BAC.

In the present study, ultrasonic treatment, one of the most powerful methods for accelerating spontaneous fibrillation *in vitro*, was used to efficiently investigate the amyloid fibrillation of keratoepithelin-derived peptides (27–30). We used the wild-type R-peptide and disease-associated C-type and H-type peptides. We demonstrated that the fibrillations of these 3 peptides were accelerated in the presence of BAC, as was the case with SDS, where the most effective concentrations were around CMC. These results indicate that the accelerating effects on fibrillation at around CMC are common to various detergents, and also suggest a possible relationship between the preservatives in eye drops and the development of corneal dystrophies.

### EXPERIMENTAL PROCEDURES

**BAC and SDS**—BAC also known as alkyl dimethylbenzylammonium chloride is a cationic surfactant with a quaternary ammonium group and an alkyl group of various chain length

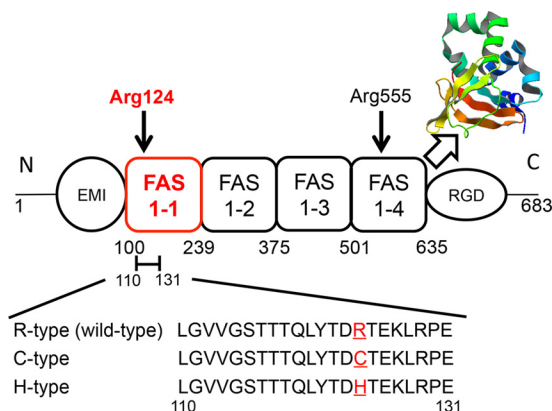


**FIGURE 1. Structural model of keratoepithelin.** The image shows a simplified diagram of keratoepithelin, which comprises cysteine-rich domain (EMI), four fasciclin 1 domains (FAS1), and an Arg-Gly-Asp (RGD) motif. Arg-124 and Arg-555 residues are hot mutations related to some corneal dystrophies. The crystal structure shows a FAS1–4 domain from human keratoepithelin (PDB ID: 2vxp). The synthesized peptides derived from the 110–131 residues of the FAS1–1 domain contain the Arg-124 residue. R124H (H-type) and R124C (C-type) mutations cause Avellino and classic lattice corneal dystrophy, respectively. R-type represents the wild-type.

(Fig. 2A,  $r = -C_8H_{17} \dots -C_{18}H_{37}$ ). In this study, we mainly used a sample with 98%  $-C_{14}H_{29}$  BAC (BAC( $C_{14}$ )) (Nacalai Tesque Inc, Kyoto, Japan) because it is most widely used as an antiseptic reagent. We also used analogues of BAC with  $C_{12}H_{25}$  (BAC( $C_{12}$ )) and  $C_{16}H_{33}$  (BAC( $C_{16}$ )) alkyl groups, which were purchased from Sigma-Aldrich. SDS, an anionic surfactant (Fig. 2B), was purchased from Nacalai Tesque Inc. (Kyoto, Japan).

**CMC**—The CMC values of BAC and SDS were determined using 8-anilino-1-naphthalenesulfonic acid (ANS), a fluorescence probe to detect water-accessible hydrophobic regions. The micelle-dependent increase in ANS fluorescence was measured with excitation and emission wavelengths of 385 nm and 475 nm, respectively, using a Hitachi spectrophotometer Model F-7000 (Hitachi, Ibaraki, Japan) (19). The reaction mixtures in 50 mM sodium phosphate buffer (pH 7.9), 100 mM NaCl, 10  $\mu$ M ANS, and various concentrations of BAC or SDS were analyzed at 37 °C after incubation for 30 min at the same temperature. The CMC values were determined from the dependence of ANS fluorescence on its concentration, where the crossing point of two linear lines represents the CMC.

**Formation of Amyloid Fibrils**—Chemically synthesized R-, H-, and C-type peptides (Fig. 1) were purchased from the Peptide Institute, Inc. (Osaka, Japan). These peptides were dissolved in a small volume of 100% dimethyl sulfoxide and left for 30 min to dissolve completely. The peptide solutions (400  $\mu$ M) were then prepared using 50 mM sodium phosphate buffer (pH 7.0) with 100 mM NaCl, 5  $\mu$ M ThT, and various concentrations (0 to 1.5 mM) of the surfactants (BAC or SDS). To accelerate fibrillation, ultrasonic pulses were applied to the peptide solutions by a water-bath-type ultrasonicator, ELESTEIN (Elekon Science Co., Ltd., Chiba, Japan) at 37 °C. The frequency of ultrasonication was near 19 kHz, and cycles of 1 min ultrasonication and 9 min quiescence were repeated (28). We also examined the effects on fibrillation of stirring the solutions with a magnetic bar at 37 °C.

In the seeding experiments, seeds were prepared by the fragmentation of preformed fibrils with a Microson XL (Misonix, Inc., Farmingdale, NY). The seeds were added at a final concentration of 20  $\mu\text{g}/\text{ml}$  to 400  $\mu\text{M}$  peptides in 50 mM sodium phosphate (pH 7.0) containing 100 mM NaCl at 37  $^{\circ}\text{C}$ .

**ThT Fluorescence Assay**—ThT specifically binds to amyloid fibrils and consequently produce enhanced light emission (18, 31, 32). The formation of amyloid fibrils was monitored with the ThT fluorescence assay using a microplate (Greiner bio-one 96-well microplate 675–074, made of polystyrene) and a microplate reader (MTP-810, Corona Electric Co., Ibaraki, Japan). Fluorescence was measured with excitation and emission wavelengths of 450 nm and 490 nm, respectively (31, 32). The lag time was defined by the time to achieve a half-maximum ThT intensity.

**Transmission Electron Microscopy**—Samples containing amyloid fibrils were diluted 10-fold with water and immediately placed on carbon-coated copper grids (400 mesh). Excess solution was removed with filter paper after the sample had stood for 1 min. The fibrils adsorbed on the grid were negatively stained with a 2% (w/v) uranyl acetate solution. Electron micrographs were acquired using a transmission electron microscope (TEM) (Hitachi, H-7650) with an acceleration voltage of 80 kV.

**Reverse-phased High Performance Liquid Chromatography (RP-HPLC) Experiments**—The C-type peptide was dissolved in a small volume of 100% dimethyl sulfoxide (DMSO) and left for 30 min to dissolve completely. 50 mM sodium phosphate buffer (pH 7.0) was then added. 20 mM dithiothreitol (DTT) was additionally added to the reduction sample to reduce disulfide bond.

Amyloid fibrils were prepared with seed-dependent fibrillation in the presence of 0.03 mM BAC or 0.7 mM SDS. The samples were centrifuged at 4  $^{\circ}\text{C}$  for 30 min (15,000 rpm) and the precipitated fibrils were recovered. 1,1,1,3,3,3-hexafluoroisopropanol (HFIP) was then added to depolymerize the fibrils and the reaction mixture was incubated at room temperature for 6 h. The depolymerized samples were analyzed by RP-HPLC with a GILSON liquid chromatogram equipped with a C4-AR-300 column (4.6  $\times$  150 nm) (Nacalai Tesque, Inc., Kyoto, Japan) at a flow rate 0.5 ml/min.

## RESULTS

**Measurement of CMCs**—SDS is a surfactant and its effects on amyloid fibrillation have been studied extensively (18–22). The effects of SDS differ significantly depending on its concentration, and concentrations of SDS around or slightly lower than CMC have been shown to generally accelerate amyloid fibrillation. In contrast, SDS higher than CMC inhibited fibrillation because of the detergent effects arising from SDS micelles (22, 23). Thus, determining the CMC value is important in evaluating the effects of a surfactant on amyloid fibrillation. The dependence of ANS fluorescence on the concentration of BAC or SDS showed a clear change in the slope, where a crossing point of the two lines represents the CMC (Fig. 2, C–F). From these plots, the CMC values for BAC(C<sub>12</sub>), BAC(C<sub>14</sub>), and BAC(C<sub>16</sub>) were determined to be 0.15, 0.02, and 0.0025 mM, respectively, in 50 mM sodium phosphate buffer (pH 7.0) containing 100 mM NaCl at 37  $^{\circ}\text{C}$ . The CMC value of SDS was also determined to be 1.0 mM under the same conditions.

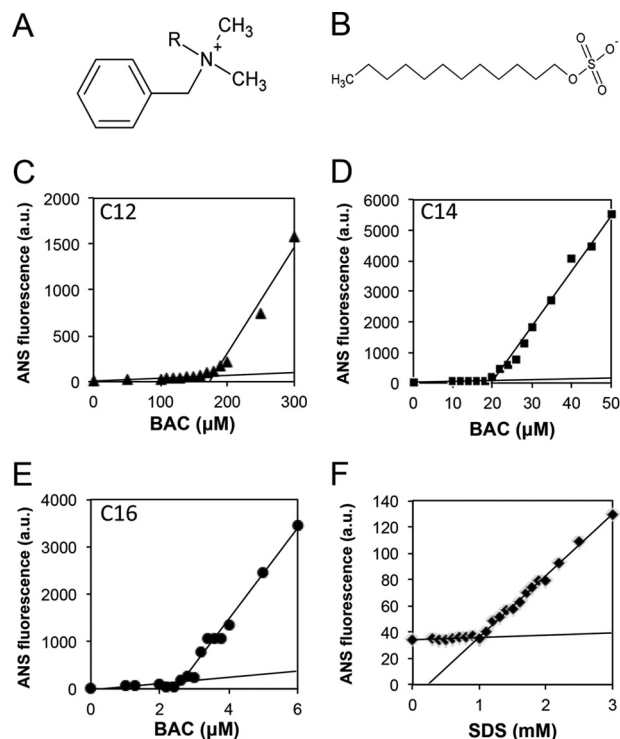


FIGURE 2. **Molecular structures and CMCs of BAC and SDS.** A and B, chemical structures of BAC (A) and SDS (B). C–F, determination of CMCs for BAC(C<sub>12</sub>) (C), C<sub>14</sub> (D), and C<sub>16</sub> (E) and SDS (F) using ANS fluorescence. The CMC values of BAC and SDS were determined to be 0.15 mM (BAC(C<sub>12</sub>)) (C), 0.02 mM (BAC(C<sub>14</sub>)) (D), 0.0025 mM (BAC(C<sub>16</sub>)) (E), and 1 mM (SDS (F)), respectively.

**Effects of BAC on Spontaneous Fibrillation**—We first examined the spontaneous fibrillation of keratoepithelin-derived peptides in the presence of various concentrations BAC(C<sub>14</sub>), the most abundant BAC in eye drops. Under quiescent conditions, the fluorescence of ThT did not significantly increase over periods of 2 weeks. Therefore, we applied ultrasonic agitations to accelerate fibrillation (28). Fig. 3, A–C show the kinetics of fibrillation of the R-, C-, and H-type peptides, respectively, in the presence of BAC(C<sub>14</sub>) at 0–1.5 mM. BAC(C<sub>14</sub>) at 0.01, 0.03, and 0.05 mM accelerated the amyloid fibrillation for all the peptides. The dependence of the final ThT fluorescence against the BAC(C<sub>14</sub>) concentration for R- and H-type peptides showed a bell-shape profile with an optimum at around CMC (0.02 mM) (Fig. 3D). In the case of the C-type peptide, the maximum ThT intensity shifted to a higher concentration of BAC(C<sub>14</sub>), suggesting that the C-type peptide was distinct from the other two peptides. We found that the fibrils of the C-type peptide were dominantly formed by dimers linked by an intermolecular disulfide bond (see below).

Interestingly, the R-type peptide formed fibrils under ultrasonic conditions, which indicates that this region of wild-type keratoepithelin exhibits amyloidogenicity regardless of the mutation. Prediction analyses suggested that aggregation propensities near the mutation site R124 were not very high and, moreover, mutations did not increase the propensity significantly (see “Discussion”). We then calculated the lag time, which represented the time required to form an amyloid nucleus, in the presence of 0–0.5 mM BAC(C<sub>14</sub>) (Fig. 3E). The lag time of all the synthetic peptides became shorter with

## BAC Induced Keratoepithelin Fibrillation

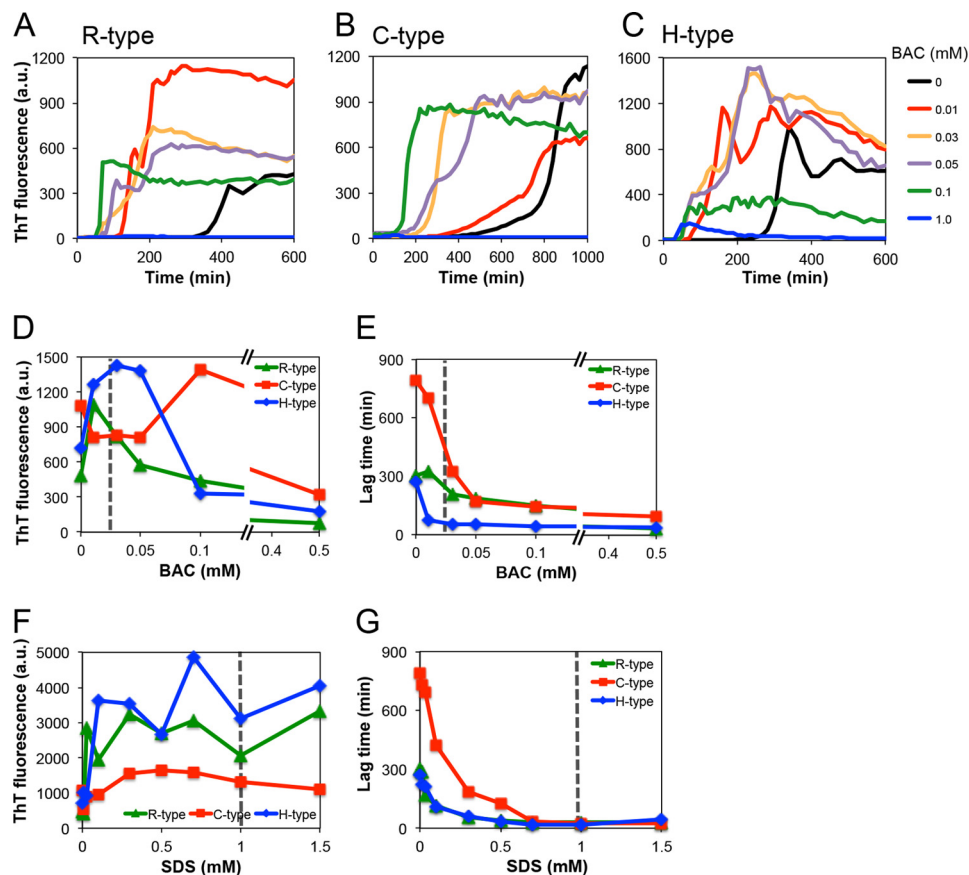


FIGURE 3. **Fibril formations of the synthetic R-, C-, and H-type peptides at various concentrations of BAC and SDS.** A–C, time courses of fibrillation at various concentrations of BAC. D and E, dependence of the amount of fibrils (D) and the lag time (E) on the BAC concentrations. F and G, dependence of the amount of fibrils (F) and the lag time (G) on the SDS concentrations.

increasing concentrations of BAC( $C_{14}$ ). These results indicate that BAC( $C_{14}$ ) accelerates the formation of amyloid nuclei in proportion to its concentration. On the other hand, high concentrations of BAC( $C_{14}$ ), especially those higher than 0.5 mM, inhibited fibrillation when monitored by ThT fluorescence. Interestingly, although the ThT fluorescence decreased, the lag time remained shorter, suggesting that the inhibition of fibrillation occurred because of the accelerated formation of amorphous aggregates at high concentrations of BAC( $C_{14}$ ). Such a competitive mechanism of amyloid fibrillation and amorphous aggregation has been proposed for the alcohol or SDS-induced amyloid fibrillation (19).

**Effects of SDS on Spontaneous Fibrillation**—We also examined the effects of SDS. A reaction mixture containing a low concentration of SDS formed amyloid fibrils within several days, even without sonication (25). With ultrasonication, amyloid fibrillation reached a plateau within several hours (data not shown). The maximum fluorescence intensity was obtained at around CMC (1.0 mM) for all types of peptides (Fig. 3F), and the lag time became shorter with increasing concentrations of SDS (Fig. 3G). Interestingly, although both cationic BAC and anionic SDS accelerated fibrillation at around their CMC, the effects of BAC( $C_{14}$ ) on the lag time were about 10-fold higher than those of SDS: The maximal concentrations of BAC( $C_{14}$ ) and SDS were 0.01 mM and 0.7 mM, respectively.

**Morphology of Spontaneously Formed Fibrils**—Fibrils observed by TEM (Fig. 4 and Fig. 5) showed that, in the absence of

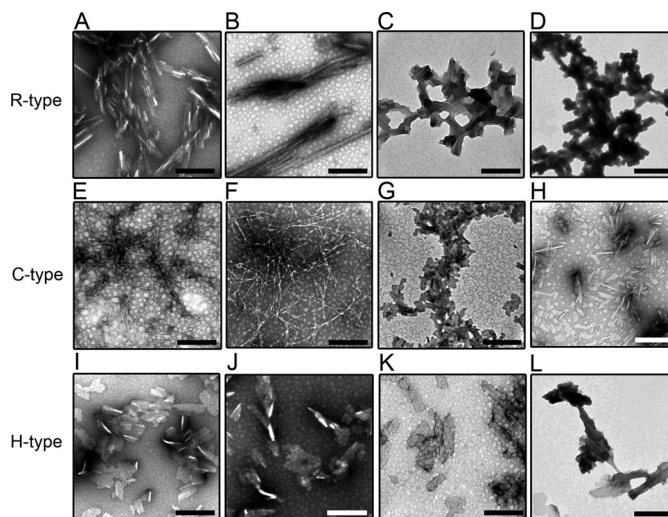


FIGURE 4. **High-magnification TEM images of the amyloid fibrils of the R- (A–D), C- (E–H), and H-type (I–L) peptides in the absence and presence of BAC.** The BAC concentrations were 0 (A, E, and I), 0.01 (B, F, and J), 0.3 (C, G, and K), and 1.5 mM (D, H, and L). When the concentration of BAC was increased, the bundles of amyloid fibrils became thicker in the R- and H-type peptides. The scale bars represent 200 nm.

BAC and SDS, the morphologies of these fibrils were distinct among the 3 peptides. The protofibrils of the R- and H-type fibrils interacted with each other to form a sheet-like morphology (Figs. 4, A, I, and 5, A, I). In the case of the C-type fibrils, thin and long rigid fibrils formed under ultrasonic conditions (Figs.

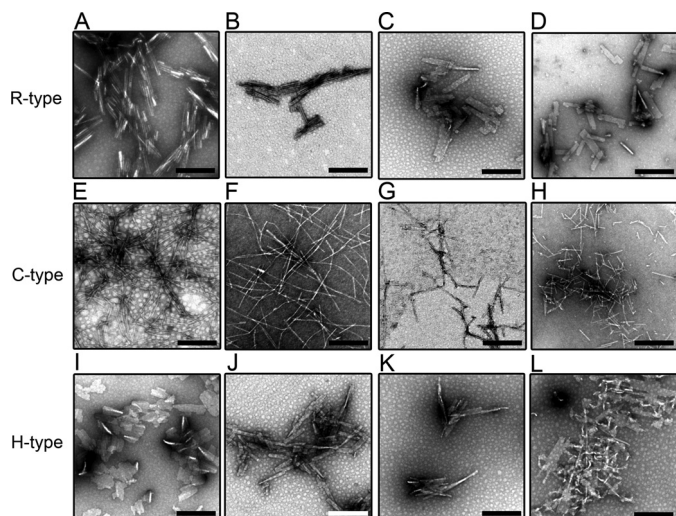


FIGURE 5. High-magnification TEM images of amyloid fibrils of the R- (A–D), C- (E–H), and H-type (I–L) peptides in the absence and presence of SDS. The SDS concentrations were 0 (A, E, and I), 0.01 (B, F, and J), 0.3 (C, G, and K), and 1.5 mM (D, H, and L). The addition of SDS did not have any significant effects on the morphology of the amyloid fibrils. The scale bars represent 200 nm.

4E and 5E). In the presence of BAC( $C_{14}$ ) at around CMC, the morphologies of the 3 types of fibrils were similar to those formed in the absence of surfactants (Fig. 4, B, F, and J). At high concentrations of BAC, the R- and H-type peptides formed sheet-like fibrils (Fig. 4, C–D and K–L). The morphologies of the fibrils made from the R- and H-type peptides were similar, independent of BAC( $C_{14}$ ) concentrations. In contrast, the C-type fibrils exhibited distinct morphologies at around and above CMC. At high concentrations of BAC( $C_{14}$ ), the C-type fibrils exhibited short and sheet-like morphologies, which were similar to those of the R- and H-type fibrils (Fig. 4, G and H). In general, fragmented fibrils were observed under ultrasonic conditions. The C-type fibrils formed at around CMC were relatively long. These images suggested that C-type fibrils have tight intermolecular interactions than those of R- and H-type fibrils.

We also performed TEM measurements of the fibrils formed in the presence of SDS (Fig. 5). In the case of R- and H-type fibrils, we obtained similar fibril images to those in the presence of BAC, which suggests that the fibrils of these peptides do not depend on the type of surfactant present (Fig. 5, B–D and J–L). In contrast, with increasing concentrations of SDS, fine fibrillar structures were seen for the C-type fibrils (Fig. 5, F–H). However, we often observed more fragmented fibrils in the TEM images obtained at high SDS concentrations than in those near CMC, which indicates that the stability of fibrils decreased at high concentrations of SDS.

**Effects of BAC Analogues with Different Alkyl Groups on Fibrillation**—Although BAC( $C_{14}$ ) is widely used as an antiseptic reagent, there are analogues of BAC with different alkyl chain length. Here, we compared the effects of 3 types of BAC analogues with  $C_{12}$ ,  $C_{14}$ , and  $C_{16}$  alkyl groups. It is noted that the effects of these BAC analogues on the cell toxicity have been examined (33). The effects of these analogues on fibrillation were examined with H-type peptide under ultrasonication (Fig. 6). For all the three types of BAC, fibrillation was

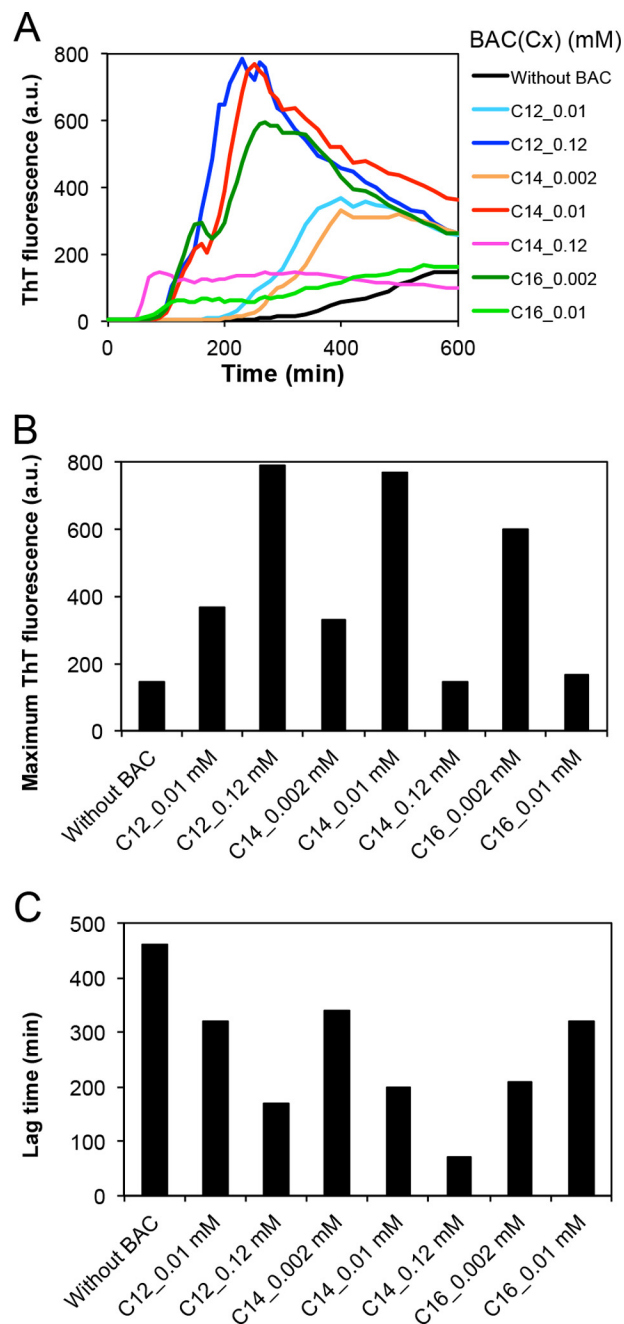


FIGURE 6. Fibril formation of the synthetic H-type peptide using BAC analogues. A, time courses of fibrillation at various concentrations of BAC( $C_{12}$ ), BAC( $C_{14}$ ), and BAC( $C_{16}$ ). B, dependence of the amount of fibrils on the concentrations of BAC( $C_{12}$ ), BAC( $C_{14}$ ), and BAC( $C_{16}$ ). C, dependence of the lag time on the concentrations of BAC( $C_{12}$ ), BAC( $C_{14}$ ), and BAC( $C_{16}$ ).

accelerated at around CMC: 0.12 mM for BAC( $C_{12}$ ), 0.01 mM for BAC( $C_{14}$ ), and 0.002 mM for BAC( $C_{16}$ ) (Fig. 6A). As described before, the CMC values for BAC( $C_{12}$ ), BAC( $C_{14}$ ), and BAC( $C_{16}$ ) were 0.15, 0.02, and 0.0025 mM, respectively. These results indicate that the optimal amyloid fibrillation around the CMC value of BAC is common to various BAC analogues with different alkyl chain length (Fig. 6, B and C).

**Seed-dependent Growth of Fibrils**—Amyloid fibrils grow without a lag phase upon the addition of fibril templates, which is called a seeding reaction. Patients with corneal dystrophies already have potential amyloid seeds due to abundant kera-

## BAC Induced Keratoepithelin Fibrillation

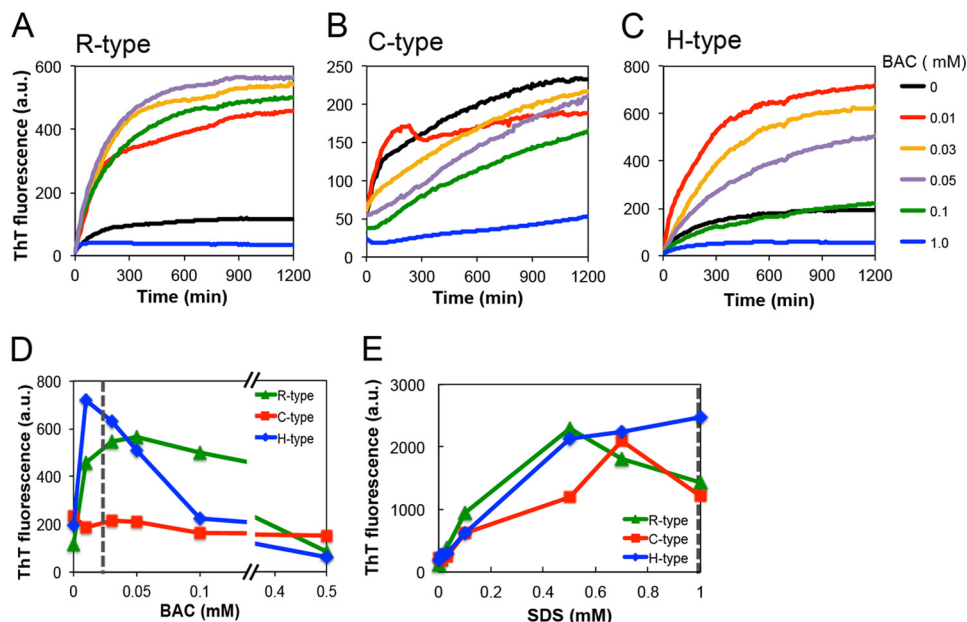


FIGURE 7. Seeding reactions of the R-, C-, and H-type peptides in the presence of various concentrations of BAC and SDS. A–C, time courses of fibrillation at various concentrations of BAC. D and E, dependence of the maximum ThT fluorescence on the BAC (D) and SDS (E) concentrations. The seeds were added at 5% (v/v) to the monomers.

toepithelin and its proteolytic products in the corneal stroma. To address the effects of BAC-containing eye drops on corneal dystrophies, we investigated *in vitro* seeding reactions. Fig. 7 shows the effects of BAC( $C_{14}$ ) on the seed-dependent fibrillation of the R-, C-, and H-type peptides. Depending on its concentration, BAC( $C_{14}$ ) accelerated the seeding reaction of the R- and H-type peptides. Concerning the R-type peptide, 0.01–0.1 mM BAC( $C_{14}$ ) accelerated the seeding reaction. At high concentrations of BAC( $C_{14}$ ) (~0.5 mM BAC( $C_{14}$ )), the accelerating effect was not evident (Fig. 7, A and D). The results of the H-type peptide were similar to those of the R-type peptide, which exhibited marked effects for 0.01–0.05 mM BAC( $C_{14}$ ) and minimal effects at higher concentrations (Fig. 7, C and D).

In contrast, the seeding reactions of the C-type peptide were distinct from the others (Fig. 7, B and D). The seeding effects were observed at all BAC( $C_{14}$ ) concentrations, except for 1.0 mM BAC( $C_{14}$ ). Additionally, the ThT intensities of several samples at time 0 were markedly high, indicating that the seeding ability of the C-type peptide was larger than that of the other peptides. This marked amyloidogenicity of the C-type peptide may have been caused by dimer formation linked by a disulfide bond (see below).

We also examined the effects of SDS on seeding reactions using the R-, C-, and H-type peptides (Fig. 7E). As was the case with BAC( $C_{14}$ ), the presence of SDS accelerated the seeding reaction, the maximum of which was observed at around CMC (1 mM).

TEM was used to observe the morphologies of fibrils formed seed-dependently in the presence of BAC (Fig. 8) or SDS (Fig. 9). All the amyloid fibrils obtained exhibited well-ordered and straight morphologies. Because the seeding reactions were performed under quiescent conditions, we did not observe the fragmented fibrils detected with the ultrasonic treatment. It appears that the addition of surfactants did not have significant

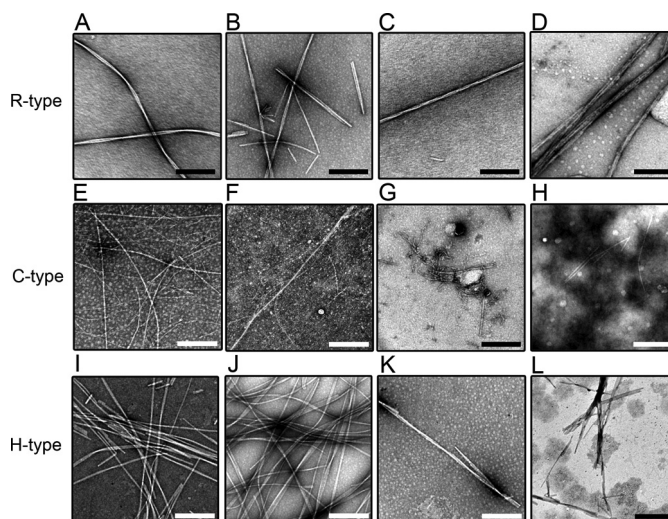
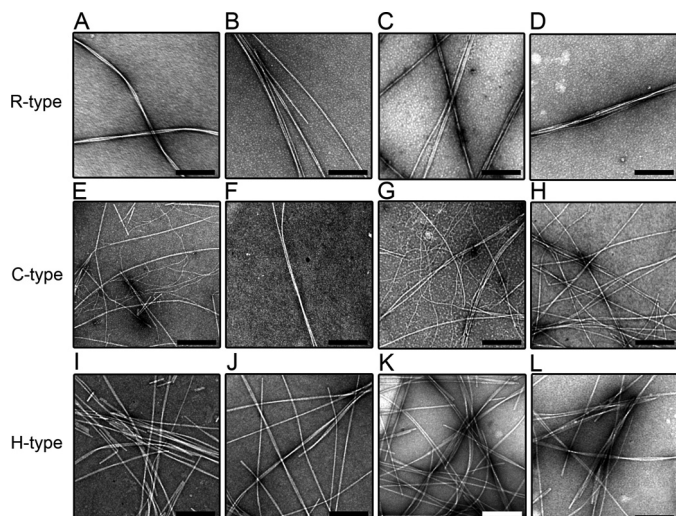


FIGURE 8. High-magnification TEM images of seed-dependent amyloid fibrils with the various concentrations of BAC. R- (A–D), C- (E–H), and H-type (I–L) peptides. BAC was added at 0 (A, E, and I), 0.01 (B, F, and J), 0.1 (C, G, and K), and 1.0 mM (D, H, and L). The scale bars represent 200 nm.

effects on the structure of amyloid fibrils. On the other hand, these surfactants accelerated the fibrillation kinetics at around CMC and also increased the amount of fibrils for all 3 types of peptides.

Our results indicate that low concentrations of BAC( $C_{14}$ ) equivalent to those present in eye drops can promote the fibrillation of both the C- and H-type peptides, associated with corneal dystrophies, as well as the wild-type R-type peptide for both spontaneous and seed-dependent fibrillations.

*Comparison of Ultrasonication and Stirring*—Although ultrasonication effectively induced the amyloid fibrillation in the presence of BAC, the effects might be specific to ultrasonication. To address the generality of the BAC effects, we examined the effects of stirring, a widely used agitation, on the fibril-



**FIGURE 9. High-magnification TEM images of seed-dependent amyloid fibrils with the various concentrations of SDS.** R- (A–D), C- (E–H), and H-type (I–L) peptides. SDS was added at 0 (A, E, and I), 0.01 (B, F, and J), 0.1 (C, G, and K), and 1.0 mM (D, H, and L). The addition of SDS did not have any significant effects on the morphology of the amyloid fibrils. The scale bars represent 200 nm.

lation of H-type peptide in the presence of BAC( $C_{14}$ ). Fibrillation of H-type peptide occurred by stirring in the presence of 0.01 mM BAC( $C_{14}$ ) (data not shown), although the effects were less than those of ultrasonication in terms of the ThT intensity. The results indicate that the BAC-dependent fibrillation is general independent of a type of agitation.

## DISCUSSION

**Effects of Surfactants on Amyloid Fibrillation**—Surfactants, in particular SDS, are known to accelerate or inhibit amyloid fibrillation depending on their concentration (18–22). The purpose of the present study was to investigate the role of BAC, the most widely used cationic surfactant, in the amyloid fibrillation of keratoepithelin-derived synthetic peptides, with a focus on the mutations found in corneal dystrophies. We observed that BAC( $C_{14}$ ), especially at a concentration around CMC (0.02 mM), accelerated both the nucleation and elongation of amyloid fibrillation for all 3 peptides (R-, C-, and H-type peptides) (Fig. 3). The acceleration of the H-type fibrillation also occurred for BAC( $C_{12}$ ) and BAC( $C_{16}$ ) indicating the generality of the BAC effects (Fig. 6).

The acceleration of amyloid fibrillation may have occurred through the direct interaction between the surfactant and peptide molecules. The binding of surfactants to the peptides occurs by the combined effects of electrostatic and hydrophobic interactions. All 3 peptides contain the same acidic amino acids (Asp and Glu) at the same position. In contrast, the R- and H-type peptides contain 3 (Arg, Lys, and His) and the C-type peptide contains 2 (Lys and Arg) basic amino acids in their sequences. The isoelectric points of the 3 peptides were 6.18 (R-), 4.68 (C-), and 5.45 (H-type) on the basis of the  $pK_a$  values of charged groups (34, 35), which indicates that, at physiological pH, the binding affinity of SDS to the C-type peptide is lower than that of the R- and H-type peptides.

Both BAC( $C_{14}$ ) and SDS accelerated the nucleation and elongation process of amyloid fibrillation (Fig. 3). However, the

acceleration by BAC( $C_{14}$ ) occurred at concentrations much lower than those by SDS. In the presence of BAC( $C_{14}$ ), the maximum amount of amyloid fibrils was detected at 0.01 mM for the H- and R-type peptides and at 0.1 mM for the C-type peptide. In contrast, the maximum amount of fibrils was detected at 0.7 mM SDS for the R- and H-type peptides and at 0.5 mM SDS for the C-type peptide. This difference in the optimal concentration is consistent with the difference in the CMC values of BAC( $C_{14}$ ) (0.02 mM) and SDS (1 mM), which confirm the importance of CMC in the mechanism of fibrillation. The optimal concentrations of BAC( $C_{12}$ ) and BAC( $C_{16}$ ) for acceleration of the H-type fibrillation were 0.12 and 0.02 mM, respectively. These values are close to their CMC values of 0.15 and 0.0025 mM, respectively, further confirming the importance of CMC (Fig. 6).

As discussed previously, when detergents exist at slightly below CMC, they start to interact with each other via hydrophobic interactions; however, the concentration is not enough to stabilize micelles. The presence of hydrophobic peptides perturbs the equilibrium by interacting with detergents, promoting the association of detergents. However, the conformational flexibility of peptides prevents the formation of ordered micelle-like structures; instead, they induce the non-organized association of a mixture of detergents and peptides, leading to amorphous aggregates and phase separation as amorphous precipitates (19, 23). However, as for some proteins and peptides, amyloid fibrils are more stable than amorphous aggregates, eventually leading to the formation of fibrils (19, 22, 23).

**Effects of Agitation on Amyloid Fibrillation**—In this study, we used ultrasonication to accelerate the amyloid fibrillation. Ultrasonic treatment is one of the most powerful methods for accelerating spontaneous fibrillation *in vitro* (30). Irradiation of an aqueous solution with ultrasonic pulses produces cavitation microbubbles that repeatedly grow and collapse in synchrony with the driving ultrasonic amplitude. The hydrophobic surface of cavitation microbubbles absorbs protein molecules, triggering the amyloid nucleation. The cavitation-induced solvent flow producing shearing force is effective to break down the preformed fibrils and thus to activate secondary nucleation.

On the other hand, more conventional method to accelerate the fibrillation is stirring the solution by a magnetic bar. The fibrillation of H-type peptide was indeed accelerated by stirring, although the effects were less than those of ultrasonication with respect to the ThT fluorescence intensity (data not shown). The results indicate that the BAC-dependent fibrillation is general independent of a type of agitation and might be possible to occur under physiological conditions, where unknown factors might trigger nucleation.

**Difference among the R-, C-, and H-type Peptides**—The reactions of the R- and H-type peptides with BAC( $C_{14}$ ) were different from those of the C-type peptide. For example, although the dependence of the lag time on the concentration of BAC( $C_{14}$ ) was similar among the 3 peptides, the lag time of the C-type peptide was about 2-fold longer than that of the R- and H-type peptides. Moreover, the maximal ThT fluorescence of the C-type peptide was observed at 0 and 0.1 mM for spontaneous and seed-dependent fibrillations, respectively, indicating the absence of a clear relationship between the maximum ThT flu-



## BAC Induced Keratoepithelin Fibrillation

orescence intensity and CMC value. The addition of BAC(C<sub>14</sub>) may have hidden the apparent effects of seeding by accelerating the overall reactions.

The high amyloidogenicity of the C-type peptide may be attributed to the formation of disulfide bonds between them. Previously, using this C-type peptide of 22-residues and a dialysis-based approach, Schmitt-Bernard *et al.* (8) reported that blocking free thiol groups to prevent the formation of disulfide bond resulted in a decrease in amyloid fibrillation. To confirm the role of disulfide linkage, we depolymerized C-type fibrils using HFIP and analyzed the oligomeric states by reverse-phased high performance liquid chromatography (data not shown). The results showed that almost all depolymerized C-type peptides assumed dimers, which indicates that the disulfide bond promotes fibrillation.

Several examples have shown that the formation of dimers and higher oligomers by disulfide linkages increased the amyloidogenicity of peptides (36, 37). Thus, the increased amyloidogenicity of disulfide linked peptides and proteins are likely to be a common property, although the biological significance in corneal dystrophies is unknown.

In addition, the net charge of the peptides is an important factor in determining the reactions between peptides and BAC, and, thus, their amyloidogenicity. His and Arg residues have a positive charge, while the Cys residue is neutral under physiological pH conditions. The more positively charged H- and R-type peptides may interact with negatively charged SDS more than the C-type peptide. On the other hand, they interact with positively charged BAC less tightly than that of the C-type peptide. These attractive interactions may decrease the concentration of monomeric detergents so as to increase the apparent CMC values.

**Comparison of *in Vitro* and *in Vivo* Models**—We anticipated that the wild-type R-type peptide would have the lowest amyloidogenicity. Interestingly, amyloid fibrillations were seen for all R-, C-, and H-type peptides. This result indicates that, in addition to the mutation, additional factors are involved in the pathogenesis of corneal dystrophies *in vivo*. Although keratoepithelin is expressed in various organs, including the skin and kidneys, amyloid fibrils were seen in the cornea only (11), which emphasizes the importance of tissue-specific additional factors.

One of these additional factors may be the post-translational processing of keratoepithelin (7, 38). Abnormal post-translational glycation, D-β-Asp racemization, and proteolysis have been shown to be involved in amyloid fibrillation in corneal dystrophies (38, 39). In addition, because many amyloidogenic sequences are buried or have a non-amyloidogenic conformation, denaturation has been suggested to make these proteins amyloidogenic. Several methods have been proposed to predict the amyloidogenic or aggregative propensities of proteins and peptides, such as TANGO (40), Zyggregator (41), AGGRESCAN (42), PASTA (43), and 3D profiling (44). A recent approach to predicting the amyloidogenicity of proteins with 3D profiling has coined the term “amylome”, and proposes that practically all human proteins contain an amyloidogenic sequence (16). We performed prediction analyses by Zyggregator (41) and AGGRESCAN (42) to compare the aggregation propensities of

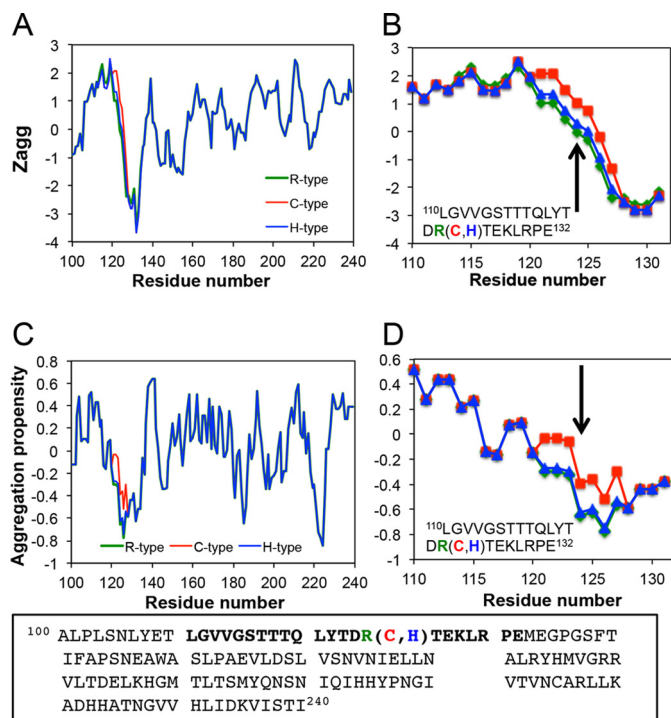


**FIGURE 10. Aggregation propensities of Fas1-1 domain of keratoepithelin.** A–D, predicted aggregation propensities by Zyggregator (41) (A and B), and AGGRESCAN (42) (C and D). The regions of synthesized peptides are expanded in B and D. The mutation site R124 is indicated by arrows.

the R-, C-, and H-type peptides (Fig. 10). The aggregation propensity near mutation site R124 was not very high. Although the aggregation propensity increased slightly upon the R to C mutation, there was no clear difference among the 3 peptides.

We still do not know the critical length of the keratoepithelin peptides in the amyloid deposits of patients as well as the entire three-dimensional structure of the intact keratoepithelin molecule (Fig. 1). It is probable that the amyloidogenicity of keratoepithelin is revealed upon the denaturation and consequent exposure of the amyloidogenic regions, and that disease-associated mutations decrease the stability of the native conformation. It is also possible that mutations affect other post-translational processes, leading to the accelerated exposure of the amyloidogenic sequence and, thus, to the development of corneal dystrophies (7, 8).

**Risk of BAC on Cornea Dystrophies**—Various antiseptic reagents, including BAC, ethyl parahydroxybenzoate, and methyl parahydroxybenzoate, are added to most commercially available eye drops. BAC(C<sub>14</sub>) is the most widely used among them because it has a broad spectrum of activity on most pathogenic microorganisms and relatively low toxic effects on the cornea (26). The concentration of BAC(C<sub>14</sub>) in eye drops is 0.001–0.02% (0.03–0.6 mM), which indicates that the maximum concentration of BAC in the cornea after instillation would be more than its CMC (0.02 mM). This finding suggests the potential risk that BAC(C<sub>14</sub>) in eye drops may accelerate amyloid fibrillation in patients with corneal dystrophies as well as in those with the potential of developing corneal dystrophies. There has been no etiological data identifying the use of BAC(C<sub>14</sub>)-containing eye drops as a deteriorating factor of corneal dystrophies. However, it would be reasonable to prescribe

BAC(C<sub>14</sub>)-free eye drops to patients, especially those with corneal dystrophies.

**Conclusion**—We investigated the *in vitro* effects of BAC(C<sub>14</sub>), an antiseptic reagent widely used in most commercially available eye drops, on amyloid fibrillation using 22-residue synthetic peptides corresponding to those found in corneal dystrophies. Using our *in vitro* system with ultrasonication for accelerated fibrillation, we identified the fibrillation of disease-associated H- and C-peptides as well as the wild-type R-peptide. These results support the views of amyloids that most proteins contain amyloidogenic sequences and that additional factors disclosing the hidden amyloidogenicity may be more important than the intrinsic amyloidogenicity of the amino acid sequence for clarifying the biological impact of amyloidogenicity.

Using the current system with ultrasonication for accelerated fibrillation, we can evaluate the effects of various reagents on amyloid fibrillation within a week. In addition to BAC(C<sub>14</sub>), each component of various eye drops should be evaluated to clarify its potential risk of amyloid fibrillation. The information obtained will be useful in selecting safer medications for patients with corneal dystrophies as well as for normal people.

## REFERENCES

- Munier, F. L., Korvatska, E., Djemai, A., Le Paslier, D., Zografos, L., Pescia, G., and Schorderet, D. F. (1997) Kerato-epithelin mutations in four 5q31-linked corneal dystrophies. *Nat. Genet.* **15**, 247–251
- Dobson, C. M. (2003) Protein folding and misfolding. *Nature* **426**, 884–890
- Stoppini, M., Andreola, A., Foresti, G., and Bellotti, V. (2004) Neurodegenerative diseases caused by protein aggregation: a phenomenon at the borderline between molecular evolution and ageing. *Pharmacol. Res.* **50**, 419–431
- Kannabiran, C., and Klintworth, G. K. (2006) TGFBI gene mutations in corneal dystrophies. *Hum. Mutat.* **27**, 615–625
- Valleix, S., Gillmore, J. D., Bridoux, F., Mangione, P. P., Dogan, A., Nedelec, B., Boimard, M., Touchard, G., Goujon, J. M., Lacombe, C., Lozeron, P., Adams, D., Lacroix, C., Maisonobe, T., Planté-Bordeneuve, V., Vrana, J. A., Theis, J. D., Giorgetti, S., Porcari, R., Ricagno, S., Bolognesi, M., Stoppini, M., Delpech, M., Pepys, M. B., Hawkins, P. N., and Bellotti, V. (2012) Hereditary systemic amyloidosis due to Asp76Asn variant  $\beta_2$ -microglobulin. *N. Engl. J. Med.* **366**, 2276–2283
- Schmitt-Bernard, C. F., Chavanieu, A., Derancourt, J., Arnaud, B., Demaille, J. G., Calas, B., and Argiles, A. (2000) *In vitro* creation of amyloid fibrils from native and Arg124Cys mutated  $\beta$ IGH3(110–131) peptides, and its relevance for lattice corneal amyloid dystrophy type I. *Biochem. Biophys. Res. Commun.* **273**, 649–653
- Korvatska, E., Henry, H., Mashima, Y., Yamada, M., Bachmann, C., Munier, F. L., and Schorderet, D. F. (2000) Amyloid and non-amyloid forms of 5q31-linked corneal dystrophy resulting from kerato-epithelin mutations at Arg-124 are associated with abnormal turnover of the protein. *J. Biol. Chem.* **275**, 11465–11469
- Schmitt-Bernard, C. F., Chavanieu, A., Herrada, G., Subra, G., Arnaud, B., Demaille, J. G., Calas, B., and Argilés, A. (2002) BIGH3 (TGFBI) Arg124 mutations influence the amyloid conversion of related peptides *in vitro*. *Eur. J. Biochem.* **269**, 5149–5156
- Yuan, C., Berscheid, H. L., and Huang, A. J. (2007) Identification of an amyloidogenic region on keratoepithelin via synthetic peptides. *FEBS Lett.* **581**, 241–247
- Korvatska, E., Munier, F. L., Djemai, A., Wang, M. X., Frueh, B., Chiou, A. G., Uffer, S., Ballestrazzi, E., Braunstein, R. E., Forster, R. K., Culbertson, W. W., Boman, H., Zografos, L., and Schorderet, D. F. (1998) Mutation hot spots in 5q31-linked corneal dystrophies. *Am. J. Hum. Genet.* **62**, 320–324
- El Kochairi, I., Letovanec, I., Uffer, S., Munier, F. L., Chaubert, P., and Schorderet, D. F. (2006) Systemic investigation of keratoepithelin deposits in TGFBI/BIGH3-related corneal dystrophy. *Mol. Vis.* **12**, 461–466
- Harrison, R. S., Sharpe, P. C., Singh, Y., and Fairlie, D. P. (2007) Amyloid peptides and proteins in review. *Rev. Physiol. Biochem. Pharmacol.* **159**, 1–77
- Abedini, A., and Raleigh, D. P. (2009) A critical assessment of the role of helical intermediates in amyloid formation by natively unfolded proteins and polypeptides. *Protein Eng. Des. Sel.* **22**, 453–459
- Lai, Z., Colón, W., and Kelly, J. W. (1996) The acid-mediated denaturation pathway of transthyretin yields a conformational intermediate that can self-assemble into amyloid. *Biochemistry* **35**, 6470–6482
- Khurana, R., Gillespie, J. R., Talapatra, A., Minert, L. J., Ionescu-Zanetti, C., Millett, I., and Fink, A. L. (2001) Partially folded intermediates as critical precursors of light chain amyloid fibrils and amorphous aggregates. *Biochemistry* **40**, 3525–3535
- Goldschmidt, L., Teng, P. K., Riek, R., and Eisenberg, D. (2010) Identifying the amyloids, proteins capable of forming amyloid-like fibrils. *Proc. Natl. Acad. Sci. U.S.A.* **107**, 3487–3492
- Raimondi, S., Guglielmi, F., Giorgetti, S., Di Gaetano, S., Arciello, A., Monti, D. M., Relini, A., Nichino, D., Doglia, S. M., Natalello, A., Pucci, P., Mangione, P., Obici, L., Merlini, G., Stoppini, M., Robustelli, P., Tartaglia, G. G., Vendruscolo, M., Dobson, C. M., Piccoli, R., and Bellotti, V. (2011) Effects of the known pathogenic mutations on the aggregation pathway of the amyloidogenic peptide of apolipoprotein A-I. *J. Mol. Biol.* **407**, 465–476
- Yamamoto, S., Hasegawa, K., Yamaguchi, I., Tsutsumi, S., Kardos, J., Goto, Y., Gejyo, F., and Naiki, H. (2004) Low concentrations of sodium dodecyl sulfate induce the extension of  $\beta_2$ -microglobulin-related amyloid fibrils at a neutral pH. *Biochemistry* **43**, 11075–11082
- Yamaguchi, K., Naiki, H., and Goto, Y. (2006) Mechanism by which the amyloid-like fibrils of a  $\beta_2$ -microglobulin fragment are induced by fluorine-substituted alcohols. *J. Mol. Biol.* **363**, 279–288
- Sureshbabu, N., Kirubakaran, R., and Jayakumar, R. (2009) Surfactant-induced conformational transition of amyloid  $\beta$ -peptide. *Eur. Biophys. J.* **38**, 355–367
- Khan, J. M., Qadeer, A., Chaturvedi, S. K., Ahmad, E., Rehman, S. A., Gourinath, S., and Khan, R. H. (2012) SDS can be utilized as an amyloid inducer: a case study on diverse proteins. *PLoS One* **7**, e29694
- Otzen, D. E. (2010) Amyloid formation in surfactants and alcohols: membrane mimetics or structural switchers? *Curr. Protein Pept. Sci.* **11**, 355–371
- Otzen, D. (2011) Protein-surfactant interactions: a tale of many states. *Biochim. Biophys. Acta* **1814**, 562–591
- Hoshino, M., Hagihara, Y., Hamada, D., Kataoka, M., and Goto, Y. (1997) Trifluoroethanol-induced conformational transition of hen egg-white lysozyme studied by small-angle X-ray scattering. *FEBS Lett.* **416**, 72–76
- Ozawa, D., Kaji, Y., Yagi, H., Sakurai, K., Kawakami, T., Naiki, H., and Goto, Y. (2011) Destruction of amyloid fibrils of keratoepithelin peptides by laser irradiation coupled with amyloid-specific thioflavin T. *J. Biol. Chem.* **286**, 10856–10863
- Mullen, W., Shepherd, W., and Labovitz, J. (1973) Ophthalmic preservatives and vehicles. *Surv. Ophthalmol.* **17**, 469–483
- Ohhashi, Y., Kihara, M., Naiki, H., and Goto, Y. (2005) Ultrasonication-induced amyloid fibril formation of  $\beta_2$ -microglobulin. *J. Biol. Chem.* **280**, 32843–32848
- So, M., Yagi, H., Sakurai, K., Ogi, H., Naiki, H., and Goto, Y. (2011) Ultrasonication-dependent acceleration of amyloid fibril formation. *J. Mol. Biol.* **412**, 568–577
- Yoshimura, Y., Lin, Y., Yagi, H., Lee, Y. H., Kitayama, H., Sakurai, K., So, M., Ogi, H., Naiki, H., and Goto, Y. (2012) Distinguishing crystal-like amyloid fibrils and glass-like amorphous aggregates from their kinetics of formation. *Proc. Natl. Acad. Sci. U.S.A.* **109**, 14446–14451
- Yoshimura, Y., So, M., Yagi, H., and Goto, Y. (2013) Ultrasonication: An Efficient Agitation for Accelerating the supersaturation-limited amyloid fibrillation of proteins. *Jpn. J. Appl. Phys.* **52**, 07HA 01:01–08
- Naiki, H., Higuchi, K., Hosokawa, M., and Takeda, T. (1989) Fluorometric determination of amyloid fibrils *in vitro* using the fluorescent dye, thioflavin T1. *Anal. Biochem.* **177**, 244–249

## BAC Induced Keratoepithelin Fibrillation

32. Biancalana, M., Makabe, K., Koide, A., and Koide, S. (2009) Molecular mechanism of thioflavin-T binding to the surface of  $\beta$ -rich peptide self-assemblies. *J. Mol. Biol.* **385**, 1052–1063
33. Adriaens, E., Dierckens, K., Bauters, T. G., Nelis, H. J., van Goethem, F., Vanparrys, P., and Remon, J. P. (2001) The mucosal toxicity of different benzalkonium chloride analogues evaluated with an alternative test using slugs. *Pharm. Res.* **18**, 937–942
34. Bjellqvist, B., Hughes, G. J., Pasquali, C., Paquet, N., Ravier, F., Sanchez, J. C., Frutiger, S., and Hochstrasser, D. (1993) The focusing positions of polypeptides in immobilized pH gradients can be predicted from their amino acid sequences. *Electrophoresis* **14**, 1023–1031
35. Bjellqvist, B., Basse, B., Olsen, E., and Celis, J. E. (1994) Reference points for comparisons of two-dimensional maps of proteins from different human cell types defined in a pH scale where isoelectric points correlate with polypeptide compositions. *Electrophoresis* **15**, 529–539
36. Ohhashi, Y., Hasegawa, K., Naiki, H., and Goto, Y. (2004) Optimum amyloid fibril formation of a peptide fragment suggests the amyloidogenic preference of  $\beta_2$ -microglobulin under physiological conditions. *J. Biol. Chem.* **279**, 10814–10821
37. Millucci, L., Paccagnini, E., Ghezzi, L., Bernardini, G., Braconi, D., Laschi, M., Consumi, M., Spreafico, A., Tanganelli, P., Lupetti, P., Magnani, A., and Santucci, A. (2011) Different factors affecting human ANP amyloid aggregation and their implications in congestive heart failure. *PLoS One* **6**, e21870
38. Kaji, Y., Oshika, T., Takazawa, Y., Fukayama, M., and Fujii, N. (2012) Co-localisation of advanced glycation end products and D- $\beta$ -aspartic acid-containing proteins in gelatinous drop-like corneal dystrophy. *Br. J. Ophthalmol.* **96**, 1127–1131
39. Kaji, Y., Oshika, T., Takazawa, Y., Fukayama, M., and Fujii, N. (2010) Accumulation of D- $\beta$ -aspartic acid-containing proteins in age-related ocular diseases. *Chem. Biodivers.* **7**, 1364–1370
40. Fernandez-Escamilla, A. M., Rousseau, F., Schymkowitz, J., and Serrano, L. (2004) Prediction of sequence-dependent and mutational effects on the aggregation of peptides and proteins. *Nat. Biotechnol.* **22**, 1302–1306
41. Tartaglia, G. G., Pawar, A. P., Campioni, S., Dobson, C. M., Chiti, F., and Vendruscolo, M. (2008) Prediction of aggregation-prone regions in structured proteins. *J. Mol. Biol.* **380**, 425–436
42. Conchillo-Solé, O., de Groot, N. S., Avilés, F. X., Vendrell, J., Daura, X., and Ventura, S. (2007) AGGRESCAN: a server for the prediction and evaluation of “hot spots” of aggregation in polypeptides. *BMC Bioinformatics* **8**, 65
43. Trovato, A., Chiti, F., Maritan, A., and Seno, F. (2006) Insight into the structure of amyloid fibrils from the analysis of globular proteins. *PLoS Comput. Biol.* **2**, e170
44. Thompson, M. J., Sievers, S. A., Karanicolas, J., Ivanova, M. I., Baker, D., and Eisenberg, D. (2006) The 3D profile method for identifying fibril-forming segments of proteins. *Proc. Natl. Acad. Sci. U.S.A.* **103**, 4074–4078

**Benzalkonium Chloride Accelerates the Formation of the Amyloid Fibrils of  
Corneal Dystrophy-associated Peptides**

Yusuke Kato, Hisashi Yagi, Yuichi Kaji, Tetsuro Oshika and Yuji Goto

*J. Biol. Chem.* 2013, 288:25109-25118.

doi: 10.1074/jbc.M113.477695 originally published online July 16, 2013

---

Access the most updated version of this article at doi: [10.1074/jbc.M113.477695](https://doi.org/10.1074/jbc.M113.477695)

Alerts:

- [When this article is cited](#)
- [When a correction for this article is posted](#)

[Click here](#) to choose from all of JBC's e-mail alerts

This article cites 43 references, 8 of which can be accessed free at  
<http://www.jbc.org/content/288/35/25109.full.html#ref-list-1>